a wide range of both impurity and thermal scattering in various proportions and magnitudes, it appears that an expression of the form ρ^n, where $n \neq 2$, is not too significant, since it breaks down over a wide range of data. The slope of 1.4 in Fig. 5 may be due to a mixture of Luttinger and Karplus-Luttinger–type terms.

An interesting correlation occurs between the quantity R_s/ρ^2 at room temperature over the whole Fe-Ni composition range, as reported by Jellinghaus and de Andres,[29] and the first magnetic anisotropy constant K_1.[30] Both are positive from iron to about 80% Ni where both change sign, and their behaviors are very similar over the whole range of compositions. This may be due to the fact that, in the Karplus-Luttinger treatment, which probably gives the dominant contribution at room temperature, R_s/ρ^2 should be proportional to the strength of the spin-orbit coupling and the anisotropy energy should have the same dependence.

[29] W. Jellinghaus and M. P. de Andres, Ann. Phys. (Leipzig), 5, 187 (1960).
[30] R. M. Bozorth, *Ferromagnetism* (D. Van Nostrand Company, Inc., Princeton, New Jersey, 1951), p. 571.

ACKNOWLEDGMENTS

We are grateful to various members of the Physics Department of Carnegie Institute of Technology, particularly to Dr. L. Berger and Dr. A. C. Ehrlich, for many helpful discussions. We are indebted to the U. S. Army Research Office (Durham) for their support of this work.

PHYSICAL REVIEW VOLUME 140, NUMBER 2A 18 OCTOBER 1965

Propagation of Bragg-Reflected Neutrons in Large Mosaic Crystals and the Efficiency of Monochromators

S. A. WERNER*
Department of Nuclear Engineering, University of Michigan, Ann Arbor, Michigan
AND
ANTHONY ARROTT
Scientific Laboratory, Ford Motor Company, Dearborn, Michigan
(Received 5 April 1965)

The general integral equations for describing the multiple Bragg reflections in a mosaic crystal are given. The solutions of the general problem are in the form of infinite series. For the particular problem of a delta-function beam striking a semi-infinite crystal, these series are summed to give modified Bessel functions as the appropriate solutions. The modified Bessel-function solution serves as a Green's function for the generation of solutions of a general beam striking a semi-infinite crystal. Discussed in some detail are the effects of absorption and of crystal-cutting angle on the efficiency of monochromating crystals. The concept of the asymptotic value of neutron current density is stressed to show the importance of not collimating the beam between the neutron source and the monochromating crystal.

I. INTRODUCTION

THE approach taken by this paper in analyzing the multiple-Bragg-scattering problem in mosaic crystals is similar to that taken by Hamilton.[1] However, the differential equations given by Hamilton describing the conservation of neutrons are recast in integral form. Consequently, the starting point of the analysis here closely parallels that given by Vineyard.[2] While the historic interest in the multiple-Bragg-scattering problem (or secondary-extinction problem) has been the need to make corrections for it in comparing intensities in determining crystallographic structure, our primary interest has been in the design of diffraction experiments to make greater use of the neutron source available at low- to medium-flux reactors.

For example, in order to obtain an acceptable resolution in doing single-crystal experiments the divergence of the "monoenergetic" beam from a monochromator must be less than of the order of 1° in the horizontal plane and perhaps 3° in the vertical plane (owing to crystal size). This implies that only those neutrons incident on the monochromator in a small solid angle of the order of 0.0006 sr are useful. This solid angle subtends only about 15 sq in. at a reactor face 12 ft away. Thus, for these small angles the reactor face looks like a plane source, and consequently, the inverse-square law does not apply. If it were possible to reflect all the neutrons in this small solid angle $\Delta\Omega$ having energies in the small spread ΔE immediately at the surface of the monochromator, we would have a plane source of "monoenergetic" neutrons which could then be colli-

* Present address: Scientific Laboratory, Ford Motor Company, Dearborn, Michigan.
[1] W. C. Hamilton, Acta Cryst. 10, 629 (1957).
[2] G. Vineyard, Phys. Rev. 96, 93 (1954).

mated between the monochromator and the target sample to produce the desired resolution at the maximum possible intensity.

In view of the fact that the absorption and incoherent scattering cross sections are small for many common monochromators, the penetration depth of the beam into the crystal is determined primarily by the probability per unit path for Bragg scattering (which is quite often 0.5 to 1 cm^{-1}). Because of this large penetration of the beam into the crystal, it is necessary to "look" inside the crystal to obtain the spatial profile of the diffracted beam at the surface of the monochromator and to find out how closely one can approximate the above idealized situation.

It is apparent that in order to "bring" the plane source of neutrons at the reactor face out a distance of 12 ft, the collimation which determines the resolution of the system must be placed between the monochromator and the target sample. Although this may seem like a simple conclusion, it is nevertheless contrary to standard practice. Since it is also desirable to use a thick monochromating crystal (when used in the Bragg position), we treat only the semi-infinite-crystal case in this paper. Problems involving crystals of finite dimensions have been solved and will be presented in a subsequent paper. It is essential here to discuss the thick-monochromator problem for the case where the incident beam is of finite size.

The inherent assumption that the extinction problem can be separated into two parts, namely, primary and secondary extinction, is present in this paper. We also assume, as has consistently been done previously, that the mosaic distribution function W depends only on orientation of the mosaics and not on the position of interest in the crystal. As has been done in the papers by Bacon and Lowde[3] (1948) and Hamilton[1] (1957), it is assumed that the displacements and distortions in the crystal which give rise to the mosaic structure are random and large compared to the wavelength of the incident neutrons, so that there are no definite phase relationships between neutrons scattered from various mosaic blocks. Consequently, we talk about current densities rather than wave functions.

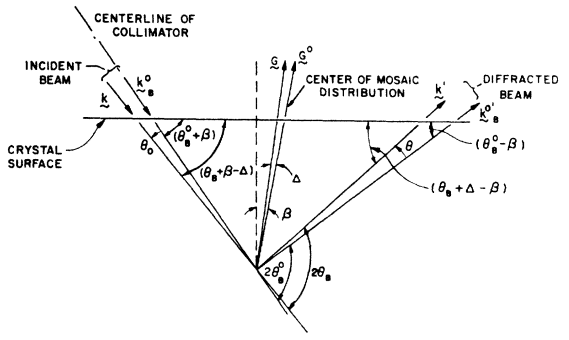

FIG. 1. Geometry of incident and diffraction directions. The wave vectors satisfy the equations: $|\mathbf{k}|\sin\theta_B=\pi|\mathbf{G}|$; $|\mathbf{k}_B{}^0|\sin\theta_B=\pi|\mathbf{G}^0|$. The angles, Δ, θ, θ_0, and Δk satisfy Eqs. (2a) and (2b). β is the angle at which the surface is cut relative to the reflecting planes.

[3] G. E. Bacon and R. D. Lowde, Acta Cryst. **1**, 303 (1948).

We define $\Sigma_s(\theta_0,k)$ to be the probability per unit path for small paths that a neutron incident on the crystal at an angle θ_0 having wave vector $\mathbf{k}$ is Bragg-reflected (Fig. 1). We also define $\Sigma_t(\theta_0,k)$ to be the probability per unit path for small paths that a neutron incident on the crystal at an angle θ_0 having wave vector $\mathbf{k}$ suffers any interaction which changes its course (including absorption). In order to obtain analytical expressions for Σ_s and Σ_t we must specify the mosaic distribution function and solve the primary extinction problem (for a small block in an infinite beam). Appendix A gives the expressions for Σ_s and Σ_t that are generally used in calculations for neutron diffraction in mosaic crystals. In the analysis which follows, it is necessary only to use the fact that if a neutron is Bragg-reflected, its course is changed by an angle $2\theta_B$ (to within a few seconds of arc). The wave vector $\mathbf{k}$, Bragg angle θ_B, and reciprocal lattice vector of interest $\mathbf{G}$ are related by

$$|\mathbf{k}|\sin\theta_B=\pi|\mathbf{G}|\,. \tag{1}$$

Neutrons which are Bragg-reflected have penetrated down into the crystal until they have reached a mosaic which is oriented at an angle such that the Bragg-Laue condition is satisfied. The incident angle θ_0, the wave-vector $\mathbf{k}$, the exit angle θ, and the mosaic angle Δ (see Appendix A and Fig. 1) are related by the equations

$$\Delta=\theta+\Delta k\,\tan\theta_B{}^0\,, \tag{2a}$$

$$\theta=\theta_0-2\Delta k\,\tan\theta_B{}^0\,, \tag{2b}$$

where $\Delta k=(|\mathbf{k}|/|\mathbf{k}_B{}^0|)-1$, $\theta_B{}^0=\sin^{-1}\pi|\mathbf{G}|/|\mathbf{k}_B{}^0|$, and $\mathbf{k}_B{}^0$ is a wave vector which lies parallel to the central ray of a collimator and satisfies the Bragg-Laue condition for mosaics lying at the center of the mosaic distribution.

II. SEMI-INFINITE CRYSTAL

A. The Multiple-Reflection Process

In order to describe the multiple reflection of neutrons in a semi-infinite crystal we first set up a pair of general integral equations which will apply to a crystal of any geometry. Consider the region R of a crystal as shown in Fig. 2. The boundary $ADBCA$ of R may be determined by the finite extent of either the beam or the crystal. The boundary is assumed to be convex with respect to $\mathbf{x}$ and $\mathbf{s}$, where the set (x,s) describes a point in a non-orthogonal coordinate system (see Fig. 2). $J_D(x,s)$ and $J_i(x,s)$ are defined as the current densities in the diffracted- and incident-beam directions, respectively.

We assume that the incident current density on the boundary curve ADB is known, and also that the diffracted current density on the boundary curve DBC is known (for example, it could be zero). J_D at any arbi-

trary point (x,s) in R is

$$J_D(x,s)=J_D(a)e^{-\Sigma_t[s-s_a(x)]}+\int_{s_a(x)}^{s}J_i(x,s')e^{-\Sigma_t(s-s')}\Sigma_s ds', \quad (3)$$

where $s_a(x)$ is the value of s at the point a, $s=s_a(x)$ is the equation of the boundary, and $J_D(a)$ is the current density in the diffraction direction at the point a on the boundary. $J_i(x,s)$ is given by

$$J_i(x,s)=J_i(b)e^{-\Sigma_t[x-x_b(s)]}+\int_{x_b(s)}^{x}J_D(x',s)e^{-\Sigma_t(x-x')}\Sigma_s dx', \quad (4)$$

where $J_i(b)$ is the incident current density at the point b on the boundary and $x_b(s)$ is the value of x at the point b. The substitution of Eq. (4) into Eq. (3) yields

$$J_D(x,s)=J_D(a)e^{-\Sigma_t[s-s_a(x)]}+\int_{s_a(x)}^{s}J_i(b')e^{-\Sigma_t[x-x_b'(s')+s-s']}\Sigma_s ds'+\int_{s_a(x)}^{s}\Sigma_s ds'\times\int_{x_b(s')}^{x}J_D(x',s')e^{-\Sigma_t(s-s'+x-x')}\Sigma_s dx'. \quad (5)$$

We define the functions $f_D(x,s)$ and $f_i(x,s)$ as

$$f_D(x,s)\equiv e^{\Sigma_t(x+s)}J_D(x,s), \quad \text{and} \quad f_i(x,s)\equiv e^{\Sigma_t(x+s)}J_i(x,s). \quad (6)$$

We then express Eq. (5) as

$$f_D(x,s)=J_D(a)e^{\Sigma_t[x+s_a(x)]}+\Sigma_s\int_{s_a(x)}^{s}J_i(b')e^{\Sigma_t[x_b(s')+s']}ds'+\Sigma_s^2\int_{s_a(x)}^{s}ds'\int_{x_b(s')}^{x}dx'f_D(x',s'), \quad (7)$$

and similarly

$$f_i(x,s)=J_i(b)e^{\Sigma_t[x_b(s)+s]}+\int_{x_b(s)}^{x}J_D(a')e^{\Sigma_t[s_a(x')+x']}\Sigma_s dx'+\Sigma_s^2\int_{x_b(s)}^{x}dx'\int_{s_a(x')}^{s}ds'f_i(x',s'). \quad (8)$$

We write Eq. (7) in the form

$$f_D=\mu_D+\Sigma_s g_D+\Sigma_s^2 L f_D, \quad (9)$$

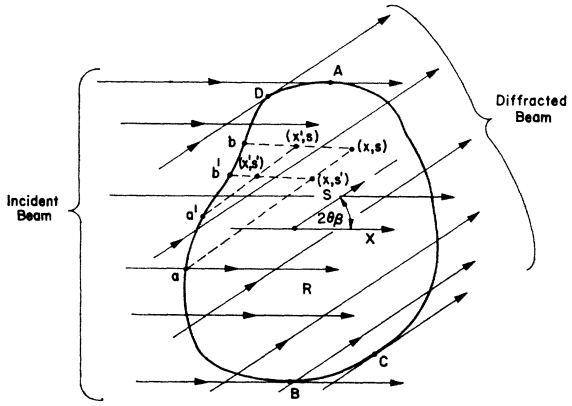

FIG. 2. Diagram of an arbitrary convex region R used in the derivation of the integral equations.

where

$$\mu_D(x,s)\equiv J_D(a)e^{\Sigma_t[x+s_a(x)]}, \quad g_D(x,s)\equiv\int_{s_a(x)}^{s}J_i(b')e^{\Sigma_t[x_b(s')+s']}ds', \quad (10)$$

(having specified J_i on the boundary ADB and J_D on the boundary DBC, g_D and μ_D are known functions) and L is a linear operator defined by

$$Lf\equiv\int_{x_b(s)}^{x}dx'\int_{s_a(x')}^{s}ds'f(x',s'). \quad (11)$$

Equation (9) may be rewritten as

$$(1-\Sigma_s^2 L)f_D=\mu_D+\Sigma_s g_D, \quad (12)$$

or

$$f_D=(1/1-\Sigma_s^2 L)(\mu_D+\Sigma_s g_D). \quad (13)$$

The same operator will appear in the corresponding expressions for f_i. In order to interpret the operator $1/(1-\Sigma_s^2 L)$ we expand it and find for the solution of Eq. (11)

$$f_D=\mu_D+\Sigma_s^2 L\mu_D+\Sigma_s^4 L^2\mu_D+\cdots+\Sigma_s g_D+\Sigma_s^3 L g_D+\Sigma_s^5 L^2 g_D\cdots, \quad (14)$$

from which

$$J_D(x,s)=e^{-\Sigma_t(x+s)}\times[\sum_{n=0}^{\infty}\Sigma_s^{2n}L^n\mu_D+\sum_{n=0}^{\infty}\Sigma_s^{2n+1}L^n g_D]. \quad (15)$$

$L^n f$ means n successive applications of the operator L to the function f. The interpretation of this solution is straightforward: The first term of the first series gives the number of neutrons which have entered R by crossing the boundary DBC in the diffraction direction **s**, and reach the point (x,s) without being reflected. The second term of the first series gives the number of neutrons which have been reflected twice and arrive at the point (x,s). The other terms in the first series are interpreted

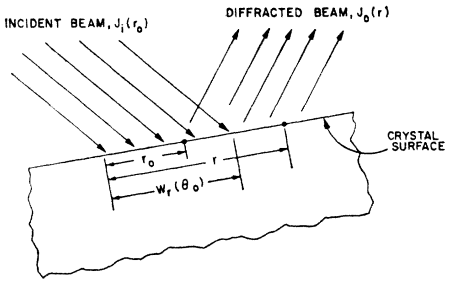

FIG. 3. Diagram showing the incident beam of effective width $w_r(\theta_0)$ impinging on a semi-infinite crystal. r_0 and r are the coordinates of the incident and diffracted beams on the surface of the crystal.

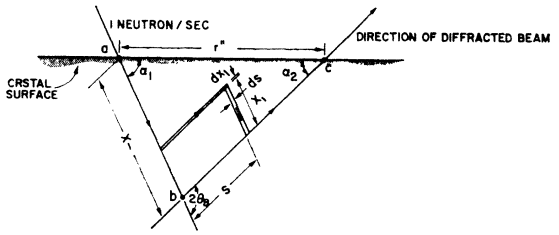

FIG. 4. Example path for a neutron entering the crystal at point a and crossing the line a-c at point c having made 3 reflections.

in a similar manner. The first term in the second series gives the number of neutrons which entered region R crossing the boundary ADB in the incident direction $\mathbf{x}$, and get to the point (x,s) via one reflection. The rest of the terms in the second series have similar meanings. Quite often μ_D is zero, so that the entire first series vanishes. This will be the case when the boundary of region R is simply the crystal surface.

The above symbolic solution to the integral equation is now applied to the special problem of a semi-infinite crystal. We describe the beam incident on a semi-infinite crystal by the distribution function $J_i(r_0,\theta_0,k)$, so that $J_i(r_0,\theta_0,k)dr_0d\theta_0dk$ is the number of neutrons incident on the crystal at the point r_0 in dr_0 at an angle θ_0 in $d\theta_0$ and having a wave vector $\mathbf{k}$ in dk.

Similarly the diffracted beam at the surface of the crystal is given by $J_D(r,\theta,k)$, where $J_D(r,\theta,k)drd\theta dk$ is the number of neutrons in the diffracted beam at the point r in dr going at an angle θ in $d\theta$, and having a wave vector $\mathbf{k}$ in dk. The coordinates r and r_0 are measured along the surface of the crystal as shown in Fig. 3. We will not change symbols for a distribution function when we change coordinates, even though the form of a function such as $J_D(r,\theta,k)$ will change if we rotate or translate the coordinate system. We think of the crystal as an operator such that

$$J_D=TJ_i. \tag{16}$$

The problem here is to find the unknown operator T. We define $G(\theta_0,k,r_0\rightarrow r)dr$ to be the probability that a neutron entering the crystal at an angle θ_0 at r_0 with wave vector $\mathbf{k}$ will leave the crystal surface at r in dr (after having been coherently scattered). Thus

$$J_D(r,\theta,k)=\int_0^r dr_0G(\theta_0,k,r_0\rightarrow r)J_i(\theta_0,k,r_0), \tag{17a}$$

where $\theta=\theta(\theta_0,k)$ is given by Eq. (2b). The wave vector and angular dependence of J_i and J_D is entirely in the dependence of Σ_s and Σ_t on these quantities. For simplicity in notation we will suppress this dependence in most of the analysis. Thus, we write

$$J_D(r)=\int_0^r dr_0G(r_0\rightarrow r)J_i(r_0), \tag{17b}$$

and will consider the problem for given k and θ_0.

To find G we let a delta-function incident beam strike the crystal at point a as shown in Fig. 4. That is, we imagine that 1 neutron/sec of a given energy and angle enters the semi-infinite crystal at point a. The region R for this problem is simply the infinite quarter-space to the right of the line $s=0$ and below the line defined by $x=(\beta_2/\beta_1)s$, where

$$\beta_1=\sin\alpha_1\approx\sin(\theta_B{}^0+\beta), \tag{18}$$

$$\beta_2=\sin\alpha_2\approx\sin(\theta_B{}^0-\beta). \tag{19}$$

The equations of the boundaries are

$$x_b(s)=(\beta_2/\beta_1)s, \tag{20a}$$

and

$$s_a(x)=0. \tag{20b}$$

The functions μ_D and g_D are

$$\mu_D=0, \tag{21a}$$

$$g_D=\int_0^s \delta(s')\left[\exp\Sigma_t\left(\frac{\beta_2}{\beta_1}s'+s'\right)\right]ds'=1, \tag{21b}$$

and the operator L takes the form

$$Lf=\int_{(\beta_2/\beta_1)s}^x dx'\int_0^s ds'f(x',s'). \tag{22}$$

Thus applying the rule given by Eq. (15) we have the diffracted current density due to an incident delta-function beam:

$${}_\delta J_D=e^{-\Sigma_t(x+s)}\sum_{n=0}^{\infty}\Sigma_s{}^{2n+1}L^ng_D$$

$$=e^{-\Sigma_t(x+s)}\left[\sum_{n=1}^{\infty}\Sigma_s{}^{2n+1}\left(\frac{x^ns^n}{n!n!}-\frac{\beta_2}{\beta_1}\frac{s^{n+1}x^{n-1}}{(n+1)!(n-1)!}\right)+\Sigma_s\right]. \tag{23}$$

This sum represents the contribution from neutrons reflected once, three times, $\cdots$, $(2n+1)$ times, $\cdots$. The spatial distribution of once-reflected neutrons is

$$ {}_sJ_D{}^{(1)}=\Sigma_s e^{-\Sigma_t(x+s)}. \tag{24}$$

For $(2n+1)$-times-reflected neutrons we have

$$ {}_sJ_D{}^{(2n+1)}=\Sigma_s{}^{2n+1}\left(\frac{x^n s^n}{n!n!}\frac{\beta_2}{\beta_1}\frac{s^{n+1}x^{n-1}}{(n+1)!(n-1)!}\right)e^{-\Sigma_t(x+s)}, \quad (n\geq 1). \tag{25}$$

A typical path taken by a 3-times-reflected neutron is shown in Fig. 4. Equation (23) can be written in terms of modified Bessel functions as

$$ {}_sJ_D=e^{-\Sigma_t(x+s)}\Sigma_s[I_0(2\Sigma_s\{xs\}^{1/2})-(\beta_2/\beta_1)(s/x)I_2(2\Sigma_s\{xs\}^{1/2})]. \tag{26}$$

A similar calculation shows that the current in the incident direction is

$$ {}_sJ_i=e^{-\Sigma_t(x+s)}\Sigma_s[(x/s)^{1/2}I_1(2\Sigma_s\{xs\}^{1/2})-(\beta_2/\beta_1)(s/x)^{1/2}I_1(2\Sigma_s\{xs\}^{1/2})]+\delta(s)e^{-\Sigma_t x}. \tag{27}$$

On the surface of the crystal we can write ${}_sJ_D$ as an expression in terms of a single variable. Figure 5 shows a coordinate y measured perpendicular to the diffracted beam, and the coordinate y_0 perpendicular to the incident beam. We express the distribution function on the surface of the crystal in terms of the variable $z=\Sigma_s y/\sin 2\theta_B=\Sigma_s x$.

$$ {}_sJ_D(z)=\left(\frac{\beta_2}{\beta_1}\right)^{1/2}\exp\left[-\frac{\Sigma_t}{\Sigma_s}\left(1+\frac{\beta_1}{\beta_2}\right)z\right]\times\left[\frac{I_1[2(\beta_1/\beta_2)^{1/2}z]}{z}\right], \tag{28}$$

where we have used Eq. (26) and the relation

$$ [I_1(2z)/z]=I_0(2z)-I_2(2z). \tag{29}$$

This function is plotted in Fig. 6 for the special case of no absorption ($\Sigma_t/\Sigma_s=1.0$) and reflecting planes parallel to the crystal surface ($\beta_1/\beta_2=1.0$). The area under ${}_sJ_D$ is 1 which means that all neutrons that enter the crystal at point a again reach the surface via single or multiple reflections in a crystal where coherent scattering is the only important interaction. (We will see that $\int_0^\infty {}_sJ_D(z)dz=1$ only when $\Sigma_t/\Sigma_s=1.0$ and $\beta_2\geq\beta_1$.)

The current density ${}_sJ_D{}^{(1)}$ due to once-reflected neutrons at the surface is a simple exponential,

$$ {}_sJ_D{}^{(1)}(z)=\exp\left[-\frac{\Sigma_t}{\Sigma_s}\left(1+\frac{\beta_2}{\beta_1}\right)z\right]. \tag{30}$$

For the case under consideration ($\Sigma_t/\Sigma_s=\beta_1/\beta_2=1.0$), the area under ${}_sJ_D{}^{(1)}$ is $\frac{1}{2}$ which shows that 50% of the total diffracted beam is accounted for by multiple reflections.

The current density due to neutrons which have been reflected three times is given by

$$ {}_sJ_D{}^{(3)}(z)=\tfrac{1}{2}\exp\left[-\frac{\Sigma_t}{\Sigma_s}\left(1+\frac{\beta_1}{\beta_2}\right)z\right]z^2\left(\frac{\beta_1}{\beta_2}\right). \tag{31}$$

This function has a maximum at

$$ z=2/[(\Sigma_t/\Sigma_s)(1+\beta_1/\beta_2)],$$

which equals one for the case under consideration. As

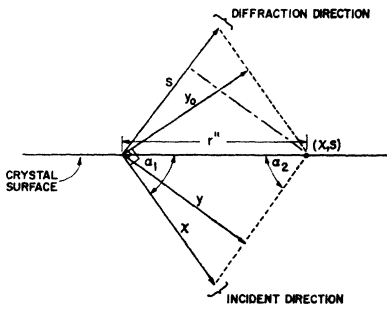

FIG. 5. Coordinate systems used in the analysis. **x** and **s** are directions of the incident and diffracted beams, respectively. $\mathbf{y}_0$ is perpendicular to **x**, **y** is perpendicular to **s**.

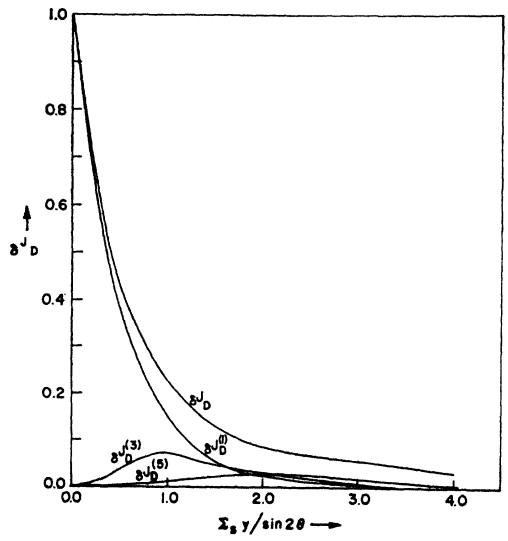

FIG. 6. Plots of the diffracted current density at the surface of a semi-infinite crystal due to an incident pencil beam. ${}_sJ_D{}^{(2n+1)}$ is the number of neutrons reaching the surface at the point corresponding to $\Sigma_s y/\sin 2\theta_B$ (see Fig. 5) after having made $(2n+1)$ reflections.

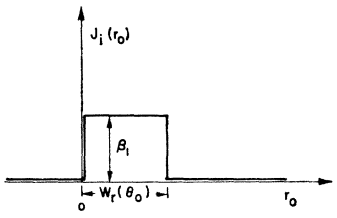

FIG. 7. Beam from a rectangular collimator as projected onto the surface of the crystal. $w_r(\theta_0)$ = effective width of the incident beam striking the crystal at an angle θ_0.

the order of multiple reflection increases, the maximum for ${}_sJ_D^{(2n+1)}(z)$ occurs at larger values of z according to

$$z_{\max}=\left[\frac{2n}{(\Sigma_t/\Sigma_s)(1+\beta_1/\beta_2)}\right]. \tag{32}$$

Multiply reflected neutrons become more important at points far out on the crystal surface away from the incident beam. A considerable fraction of the total diffracted power occurs under the tail of ${}_sJ_D$. For large z, ${}_sJ_D$ varies as $z^{-3/2}$ which is not the rapidly decreasing type of function generally associated with a coherent peak.

Equation (28), written as a distribution function in $r''=r-r_0$ (as shown in Fig. 4), is the Green's function we have sought, that is,

$$G[r-r_0]=Ae^{-C(r-r_0)}\times\frac{I_1[B(r-r_0)]}{(r-r_0)}, \tag{33}$$

where

$$A=(\beta_2/\beta_1)^{1/2},\quad B=2\Sigma_s(\beta_1\beta_2/\sin^2 2\theta_B)^{1/2}, \tag{34}$$

and

$$C=\Sigma_t((\beta_1+\beta_2/\sin 2\theta_B)).$$

B. Integration of the Green's Function

To find the diffracted beam due to an incident beam of given k and θ_0 from a rectangular collimator as shown in Fig. 7, we use Eq. (17). We have then to carry out the integration. As $G(r_0\rightarrow r)$ is a function of $(r-r_0)$, we have a convolution integral and can write Eq. (17) in the form

$$\bar{J}_D(p)=\bar{G}(p)\bar{J}_i(p). \tag{35}$$

The bar indicates that a Laplace transformation has been performed (p is the Laplace variable). $\bar{G}(p)$ is given by

$$\bar{G}(p)=A\frac{(p+B+C)^{1/2}-(p-B+C)^{1/2}}{(p+B+C)^{1/2}+(p-B+C)^{1/2}}, \tag{36a}$$

and

$$\bar{J}_i(p)=\beta_1/p. \tag{36b}$$

To obtain the diffracted current density we perform the inversion

$$J_D(r)=\mathcal{L}^{-1}\left[\frac{\beta_1 A}{p}\frac{(p+B+C)^{1/2}-(p-B+C)^{1/2}}{(p+B+C)^{1/2}+(p-B+C)^{1/2}}\right]$$
$$-\mathcal{L}^{-1}\left[e^{-W_r p}\frac{\beta_1 A}{p}\frac{(p+B+C)^{1/2}-(p-B+C)^{1/2}}{(p+B+C)^{1/2}+(p-B+C)^{1/2}}\right]. \tag{37}$$

The inversion of the first term gives a function which is zero at $r=0$ and rises as sketched in Fig. 8(a). Since $e^{-W_r p}$ is the shift operator, the inversion of the second term gives the same function as the first term only shifted to the right by an amount W_r as shown in Fig. 8(a). We call the inversion of the first term $N_D(r)$. $N_D(r)$ corresponds to the diffracted current density that would be observed for a semi-infinite beam (i.e., for $W_r\rightarrow\infty$). Thus, the current density due to a collimator of finite width is

$$J_D(r)=N_D(r)-N_D(r-W_r)\mu_{-1}(W_r). \tag{38}$$

$\mu_{-1}(W_r)$ is the unit step function shown in Fig. 8(b). This result is easily understood physically: The current density builds up from the origin; its value at a point $r\leq W_r$ is due to a contribution from all incident neutrons which enter the crystal between zero and r and reach the surface at the point r via single or multiple reflections; the larger the value of r, the greater the source of neutrons which contributes to $J_D(r)$; the curve continues to rise. At the point $r=W_r(\theta_0)$ (which is the effective width of the collimator for neutrons entering the crystal at an angle θ_0) the additional contribution to the incident source of neutrons ends, and $J_D(r)$ falls, ultimately to zero. (If $W_r\rightarrow\infty$, the "build-up" curve $N_D(r)$ would tend to an asymptotic value.)

We give here the inversion of $\bar{J}_D$ without the details of proof. Since a distribution function in terms of the variable y (measured perpendicular to the diffracted beam) is probably more meaningful than a distribution

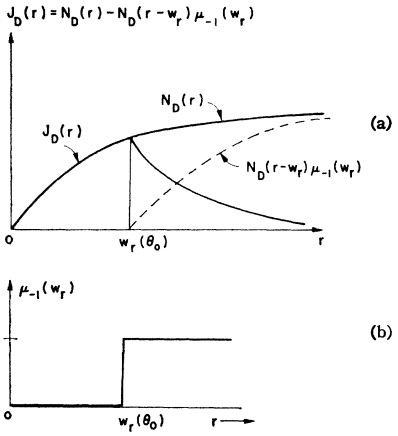

FIG. 8. (a) A sketch of $J_D(r)$ as a function made up of two parts: $N_D(r)$ and $N_D(r-w_r)\mu_{-1}(w_r)$. (b) The unit step function $\mu_{-1}(w_r)$.

function in r, the result is given in terms of $N_D(y)$,

$$N_D(y)=f_D(y)\exp\left[-\frac{\Sigma_t}{\Sigma_s}\left(1+\frac{\beta_1}{\beta_2}\right)\frac{\Sigma_s y}{\sin 2\theta_B}\right], \quad (39a)$$

where

$$f_D(y)=\left(\frac{\beta_1}{\beta_2}\right)^{1/2} I_1\left[2\left(\frac{\beta_1}{\beta_2}\right)^{1/2}\frac{\Sigma_s y}{\sin 2\theta_B}\right]+\sum_{n=2}^{\infty}\left(\frac{\beta_1}{\beta_2}\right)^{1/2}$$

$$\times[f^{n-1}+f^{-n+1}]I_n\left[2\left(\frac{\beta_1}{\beta_2}\right)^{1/2}\frac{\Sigma_s y}{\sin 2\theta_B}\right], \quad (39b)$$

and

$$f=\lambda+(\lambda^2-1)^{1/2},$$

$$\lambda=\frac{1}{2}\frac{\Sigma_t}{\Sigma_s}\left[\left(\frac{\beta_1}{\beta_2}\right)^{1/2}+\left(\frac{\beta_2}{\beta_1}\right)^{1/2}\right]. \quad (39c)$$

We note that when $\Sigma_t/\Sigma_s=1.0$ (no absorption) and $\beta_1/\beta_2=1.0$ (symmetric case), this expression reduces to

$$N_D(y)=1-e^{-2z}[I_0(2z)+I_1(2z)], \quad (40)$$

where as before $z=\Sigma_s y/\sin 2\theta_B$.

C. The Effect of the Angle β at which the Crystal is Cut Relative to the Reflecting Planes

It has been known for quite some time that when reflection takes place in the first few millimeters of the crystal (as is the case for x-ray diffraction), an apparent intensification of the diffracted beam occurs when the crystal surface is cut at an angle β relative to the reflecting plane.[4] The reason for this is apparent from Fig. 9, where the effective widths of the diffracted and incident beams stand in the approximate ratio

$$(W/W_0)[\theta_0]=\beta_2/\beta_1. \quad (41)$$

For most crystals used for monochromators in neutron-diffraction work, the coefficient of absorption is small and the beam penetrates quite deeply into the crystal. In this case it is necessary to examine the problem in more detail to determine the effect of various choices for

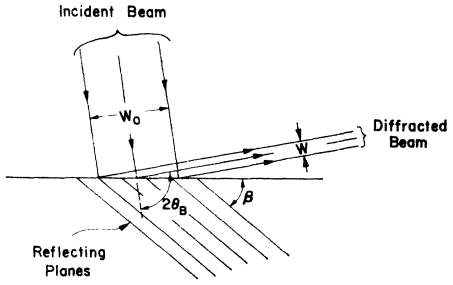

FIG. 9. The effect of cutting the crystal at an angle β relative to the reflecting planes in the event that the beam does not penetrate deeply into the crystal. There is a condensation of the effective width w_0 to w giving the apparent result that the diffracted current density is increased.

[4] I. Fankuchen, Nature **139**, 193 (1937).

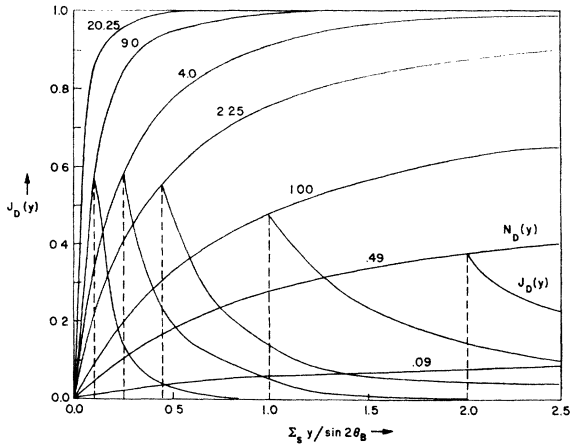

FIG. 10. "Build-up" curves for various values of β_1/β_2. The point at which the discontinuity in $J_D(y)$ occurs corresponds to the "effective" right edge of a collimator of width w.

cutting the crystal. We consider first the effect on $N_D(y)$ from which one can deduce $J_D(y)$ for various collimator parameters.

Plots of $N_D(y)$ for the case $\Sigma_t/\Sigma_s=1.0$ are given in Fig. 10. The striking increase in the rate at which the curves rise toward their asymptotic values as β_1/β_2 is increased leads one to believe that it is quite advantageous to cut the crystal at an angle such that the diffracted beam leaves the crystal in a direction almost parallel to the crystal surface. Note, however, that for a given collimator the total number of neutrons diffracted from the crystal decreases with increasing β_1/β_2 because of the narrowing of the beam. Consequently, the optimum angle at which to cut the crystal is not a simple question.

Cutting the crystal at an angle β *does not* intensify the incident beam. It simply makes $J_D(y)$ reach its asymptotic values at smaller y. The current density $J_D(y)$ is always less than the incident current density $J_i(y_0)$ which we have set equal to one. (All this is in accord with the second law of thermodynamics.)

Since the effective width of the collimator $W(\theta_0)$ as projected into a plane perpendicular to the direction of the diffracted beam is related to the effective width of the incoming beam by Eq. (41), we note that the point $[\Sigma_s W(\theta_0)/\sin 2\theta_B]$ on the curves in Fig. 10 approaches zero as β_1/β_2 increases. $[\Sigma_s W(\theta_0)/\sin 2\theta_B]$ gives the point on the crystal surface at which the "break-point" in $J_D(y)$ occurs. At this point $J_D(y)$ begins to fall off as shown in Fig. 10, where we have taken $(\Sigma_s W_0/\sin 2\theta_B)=1.0$ for purposes of illustration. It is apparent from these curves that the area under $J_D(y)$ decreases with increasing β_1/β_2 when $\beta_1/\beta_2 \geq 1.0$ even though the maximum point of $J_D(y)$ increases with β_1/β_2.

From Eq. (53) below it follows that as $(\beta_1/\beta_2)\to 0$, the peak of $J_D(y)$ goes to $1-\exp[-\Sigma_s W_0/\sin 2\theta_B]$ $(=0.632$ for the case treated here). The area under the curve for $J_D(y)$ will be the asymptotic value of $N_D(y)$

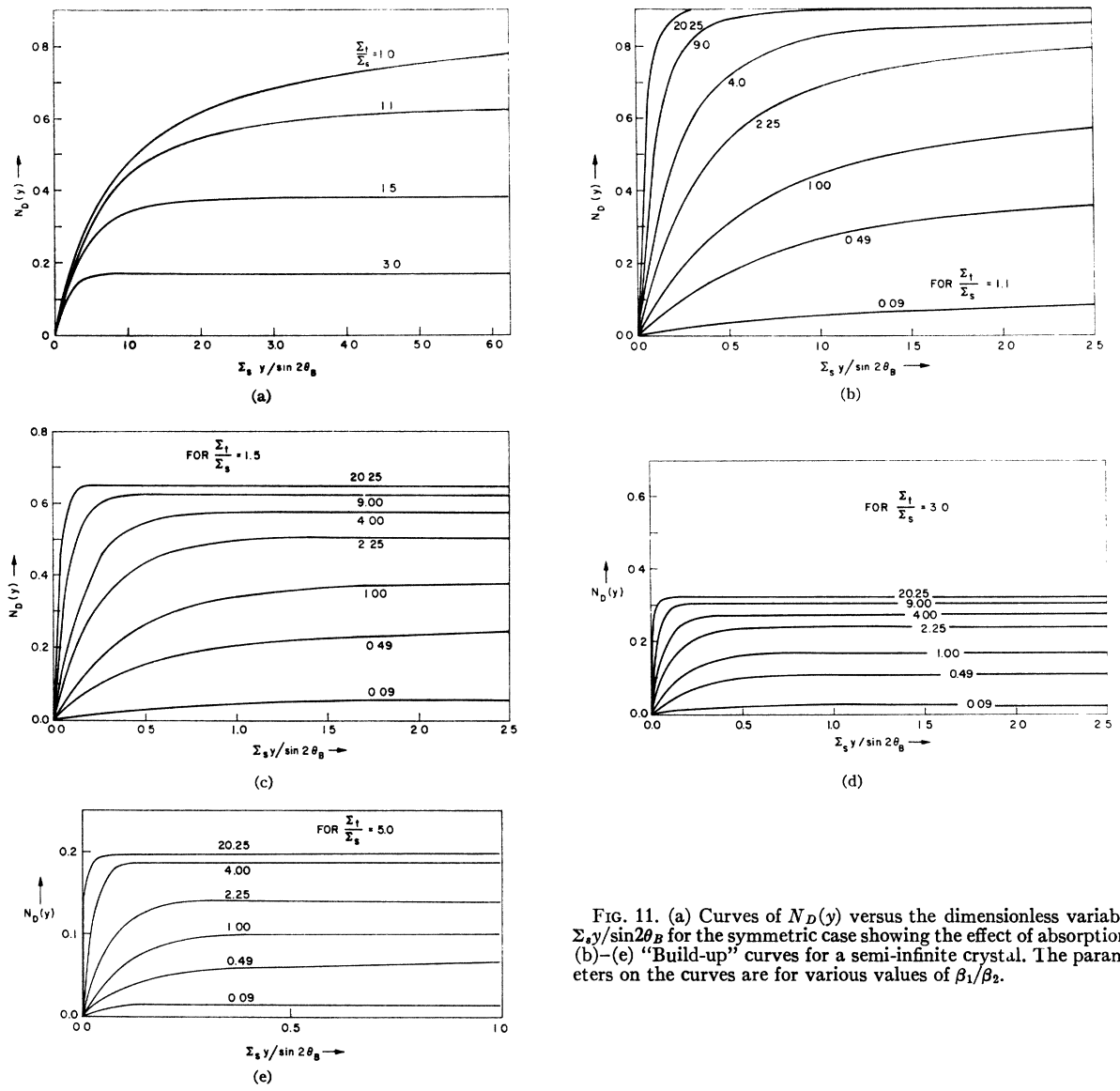

FIG. 11. (a) Curves of $N_D(y)$ versus the dimensionless variable $\Sigma_s y/\sin 2\theta_B$ for the symmetric case showing the effect of absorption. (b)–(e) "Build-up" curves for a semi-infinite crystal. The parameters on the curves are for various values of β_1/β_2.

times the "effective" width of the diffracted beam, $W = W_0(\beta_2/\beta_1)$. This is apparent from Fig. 8(a) as the two curves are displaced by W. Note that from Eq. (48) below, $N_D(\text{asymptotic}) = \beta_1/\beta_2$ for $\beta_2/\beta_1 > 1$, hence the area under the curve for $J_D(y)$ (total number of diffracted neutrons leaving the crystal) is constant and equal to the total number of neutrons incident on the crystal; whereas for $\beta_2/\beta_1 < 1$, the area gives only a fraction of the total incident beam, namely β_2/β_1.

Figures 11(a)–(e) indicate that a small amount of absorption affects the total reflection in a marked manner. Σ_t/Σ_s may be very close to 1.0 for incident neutrons which have a wave vector $\mathbf{k}$ that satisfies the Bragg condition for the part of the mosaic distribution lying at or near $\Delta = 0$, but $(\Sigma_t/\Sigma_s)(\Delta)$ rapidly becomes greater than one as $|\Delta|$ increases if there is any absorption at all.

Figures 13(a)–(c) show the effect on the distribution $\int J_D d\theta$, $\int J_D dk$, and $\int\int J_D d\theta dk$ of cutting the crystal at various angles for a particular set of system parameters as shown in Fig. 12: W_0 = actual collimator width = 1 cm; L = collimator length = 100 cm; D = distance from source plane to crystal = 150 cm; $Q = 0.01$ cm (defined in Appendix A); η = mosaic spread parameter (see Appendix A) = 15 minutes of arc; E_p = primary extinction coefficient = 1.0; $\Sigma_t/\Sigma_s = 1.0$ (no absorption); θ_B = Bragg angle = 20°.

The mosaic distribution function was assumed to be Gaussian and the walls of the collimator to be nonreflecting. The narrowing of the beam and the increasing

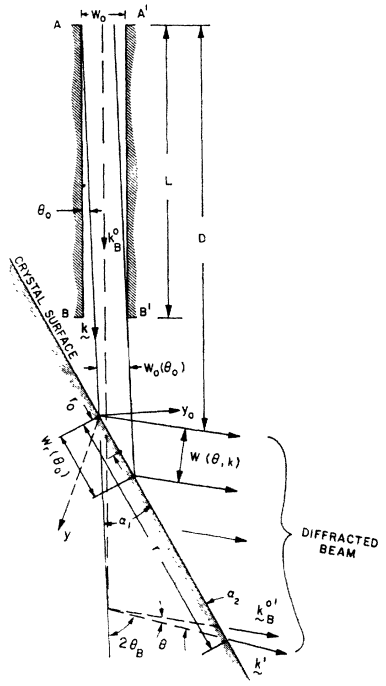

FIG. 12. Geometry of a beam from a rectangular collimator impinging on a semi-infinite crystal.

of the peak height as β is increased is quite pronounced. These integrated current densities show the expected skewing toward the right past the peak which occurs near the "effective" right edge of the collimator.

D. Asymptotic Values of the Current Density, $N_D(y)$

In this paragraph we wish to calculate $\lim_{y\to\infty} N_D(y)$ on the surface of the crystal. Rather than evaluate Eq. (39a) directly, we consider the total power equations used by Darwin,[5] Zachariasen,[6] and Bacon and Lowde[3] for an incident beam impinging on a crystal of infinite surface, namely

$$\frac{dP_i}{dh}=-\frac{\Sigma_t}{\beta_1}P_i+\frac{\Sigma_s}{\beta_2}P_D, \tag{42}$$

$$-\frac{dP_D}{dh}=-\frac{\Sigma_t}{\beta_2}P_D+\frac{\Sigma_s}{\beta_1}P_i, \tag{43}$$

where h is a perpendicular distance into the crystal. $P_i(h)$ = total power in the incident beam at a depth h, and $P_0(h)$ = total power in the diffracted beam at a depth h. These equations are solved for $P_D(h)$ subject to the boundary conditions $P_i(h=0)=P_0$, $P_D(h=T)=0$, where T is the thickness of the crystal. We are interested here in the limit as T goes to infinity. For this it is an easy matter to show that

$$\lim_{T\to\infty}\left(\frac{P_D(0)}{P_0}\right)=\left\{\frac{1}{2}\frac{\Sigma_t}{\Sigma_s}+\frac{1}{2}\frac{\Sigma_t}{\Sigma_s}\frac{\beta_1}{\beta_2}\times\left[\left(\frac{\Sigma_t}{\Sigma_s}\right)^2\left(1+\frac{\beta_1}{\beta_2}\right)^2-4\left(\frac{\beta_1}{\beta_2}\right)\right]^{1/2}\right\}^{-1}. \tag{44}$$

If the point of observation r on the crystal surface is far from the origin, $N_D(r)$ will be independent of whether the incident beam is semi-infinite or infinite. For large r, the quantity $N_D^\infty(r)$ will be a constant independent of r. $N_D^\infty(r)$ is proportional to the diffracted power for the infinite-beam case:

$$\lim_{T\to\infty}\frac{P_D(0)}{P_0}=\frac{\int N_D^\infty(r)dr}{\int N_i^\infty(r_0)dr_0}=\frac{N_D^\infty(r)}{N_i^\infty(r_0)}. \tag{45}$$

Changing variables from r to y and r_0 to y_0 (Fig. 5) gives

$$\frac{N_D^\infty(y)}{N_i^\infty(y_0)}=\frac{\beta_1}{\beta_2}\lim_{T\to\infty}\frac{P_D(0)}{P_0}. \tag{46}$$

Normalizing the incoming current density to unity when measured perpendicular to the incoming beam, we have

$$N_D(\text{asymptotic})=\frac{\beta_1}{\beta_2}\left\{\frac{1}{2}\frac{\Sigma_t}{\Sigma_s}+\frac{1}{2}\frac{\Sigma_t\beta_1}{\Sigma_s\beta_2}+\left[\left(\frac{\Sigma_t}{\Sigma_s}\right)^2\left(1+\frac{\beta_1}{\beta_2}\right)^2-4\frac{\beta_1}{\beta_2}\right]^{1/2}\right\}^{-1}, \tag{47}$$

where

$$N_D(\text{asymptotic})\equiv\lim_{y\to\infty}N_D(y)=N_D^\infty(y).$$

This function is plotted in Fig. 14 versus Σ_t/Σ_s for various values of β_1/β_2. These values are verified in the curves of Fig. 11(a)–(e). It is instructive to consider the case of no absorption ($\Sigma_t/\Sigma_s=1.0$) for which

$$\begin{aligned} N_D(\text{asymptotic})&=1 \quad \text{for} \quad \beta_1/\beta_2\geq 1,\\ &=\beta_1/\beta_2 \quad \text{for} \quad \beta_1/\beta_2<1 \end{aligned} \tag{48}$$

while the total diffracted power is

$$\begin{aligned} P_D(0)&=P_0 \quad \text{for} \quad \beta_1/\beta_2<1.\\ &=\beta_2/\beta_1 P_0 \quad \text{for} \quad \beta_1/\beta_2\geq 1 \end{aligned} \tag{49}$$

Therefore, when the diffracted beam becomes more and more nearly parallel to the crystal surface, fewer and fewer neutrons again reach the surface to appear in the diffracted beam, even though the current density reaches 1 at small values of y [see Figs. 15(a), 15(b)]. In the case when $\beta_2<\beta_1$, many of the incident neutrons do not appear in the diffracted beam at the surface of the crystal. Since they cannot disappear in a nonabsorbing

[5] G. G. Darwin, Phil. Mag. 43, 800 (1922).
[6] W. H. Zachariason, *X-Ray Diffraction in Crystals* (John Wiley & Sons, Inc., New York, 1944).

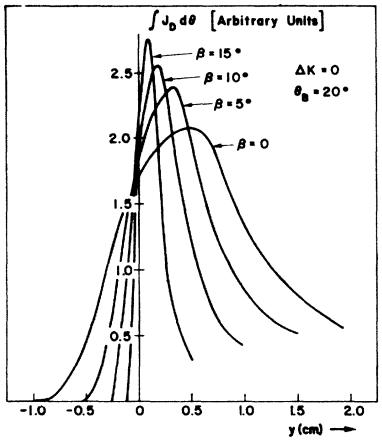

(a)

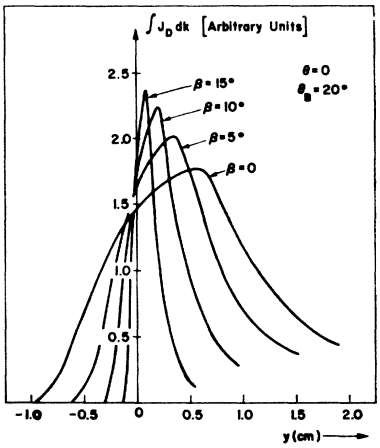

(b)

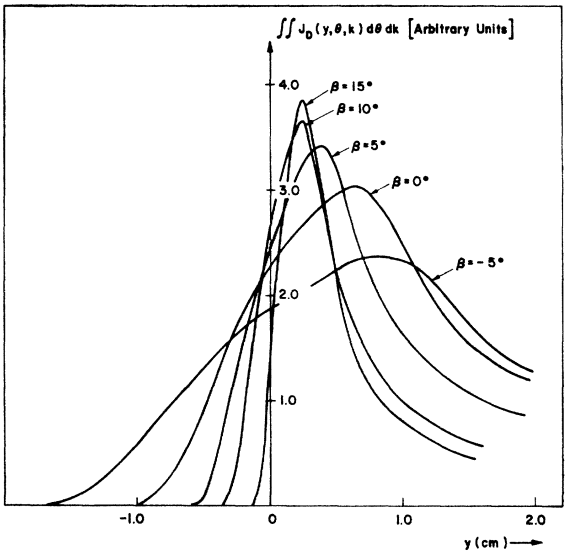

(c)

FIG. 13. (a) Spatial distribution of the integrated current $\int J_D d\theta$ for various values of β (system parameters given in the text). (b) Spatial distribution of the integrated current $\int J_D dk$ for various values of β. (c) Spatial distribution of the integrated current $\int\int J_D dk d\theta$ for various values of β.

crystal, there must be a current at infinity in the incident direction. Careful calculation shows this to be the case in evaluating $\lim_{T\to\infty} P_i(T)$. We get

$$\lim_{T\to\infty} P_i(T) = P_0(1-\beta_2/\beta_1) \quad \text{for} \quad \beta_2 \leq \beta_1, \qquad = 0 \quad \text{for} \quad \beta_2 > \beta_1. \tag{50}$$

E. Various Orders of Multiple Reflections

In this section we again consider the contributions to the diffracted current density $N_D(x,s)$ for a uniform flux of neutrons [$N_i(y_0)=1$, for $y_0 \geq 0$; that is, for an infinitely wide collimator whose left edge is at $s=0$] impinging on a semi-infinite crystal. Here, however, we inquire as to the contribution from the neutrons classified according to the number $(2k+1)$ of reflections they undergo. That is,

$$\sum_k N_D{}^{2k+1}(x,s) = N_D(x,s). \tag{51}$$

We use Eq. (25) but replace x and s by $x-x'$ and $s-s'$, where x' and s' are the coordinates of the point at which a neutron enters the crystal. For the points (x,s) and (x',s') on the crystal surface we have $(x-x')=\beta_2/\beta_1 \times(s-s')$. With this relation, ${}_\delta J_D{}^{(2k+1)}$ becomes

$${}_\delta J_D{}^{(2k+1)} = e^{-A(s-s')} \frac{\Sigma_s{}^{2k+1}(\beta_2/\beta_1)^k (s-s')^{2k}}{k!(k+1)!}, \tag{52}$$

where

$$A = \Sigma_t(\beta_2/\beta_1+1).$$

We have

$$N_D{}^{(2k+1)}(y) = \int_0^s {}_\delta J_D{}^{(2k+1)},$$

where $s=(\beta_1/\beta_2)y/\sin 2\theta_B$ for points on the crystal surface. Thus, the number of once-reflected neutrons as a

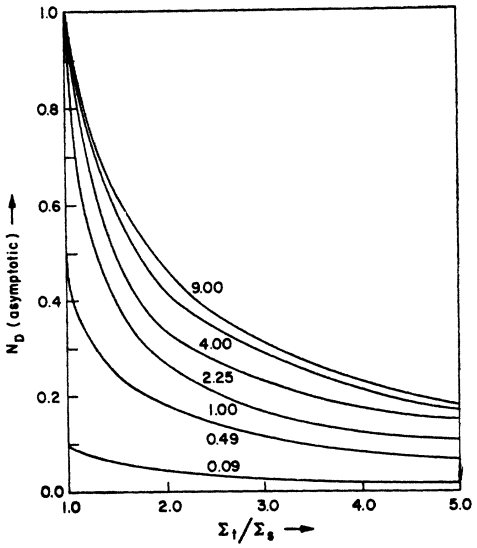

FIG. 14. Asymptotic value of the diffracted current density, $\lim(y\to\infty)N_D(y)$ as a function of Σ_t/Σ_s. The parameter on the curves is $\beta_1/\beta_2=\sin(\theta_B+\beta)/\sin(\theta_B-\beta)$.

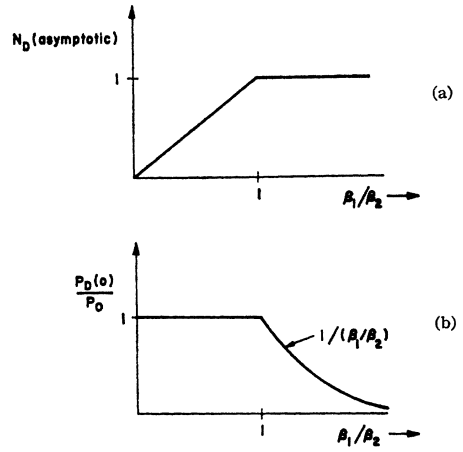

FIG. 15. (a) Asymptotic value of $N_D(y)$ when $\Sigma_t/\Sigma_s=1$ showing that the density goes to one when $\beta_2\leq\beta_1$. (b) Total reflected power from a semi-infinite crystal when $\Sigma_t/\Sigma_s=1.0$. This curve shows that all of the neutrons do not return to the surface when $\beta_2<\beta_1$, and consequently there must be a current in the incident direction at an infinite depth in the crystal.

function of y is

$$N_D^{(1)}(y)=(1-e^{-Mq})/M\,, \tag{53}$$

where $M=(\Sigma_t/\Sigma_s)[(\beta_2/\beta_1)+1]$ and $q=\Sigma_s s$.

The number of three-times reflected neutrons is

$$N_D^{(3)}(y)=\frac{1}{2}\frac{\beta_2}{\beta_1}\left[\frac{2}{M^3}-e^{-Mq}\left(\frac{q^2}{M}+\frac{2q}{M^2}+\frac{2}{M^3}\right)\right]. \tag{54}$$

In general

$$N_D^{(2k+1)}(y)=(k!(k+1)!)^{-1}(\beta_2/\beta_1)^k f_{2k}\,, \tag{55}$$

where f_{2k} satisfies the recurrence relation

$$f_{2k}=(2k(2k-1)/M^2)f_{2k-2} -(2k/M^2)q^{2k-1}e^{-Mq}-M^{-1}q^{2k}e^{-Mq}. \tag{56}$$

$N_D^{(1)}(y)$, $N_D^{(3)}(y)$, $N_D^{(5)}(y)$ are plotted in Fig. 16 for the symmetric case with no absorption. We note that for small values of y, $N_D^{(1)}(y)$ closely approximates $N_D(y)$. However, for larger values of y, $N_D(y)\to 1$, as $N_D^{(1)}(y)\to\frac{1}{2}$, and the higher orders of multiple reflection sum to give 50% of the intensity.

There are three cases in which once-reflected neutrons dominate the asymptotic values of $N_D(y)$. These are when $\beta_1/\beta_2\to 0$, $\beta_2/\beta_1\to 0$, and for strong absorption. We have asymptotically

$$N_D^{(2k+1)}(\text{asymptotic})=(k!(k+1)!)^{-1} \times(\beta_2/\beta_1)^k(2k!/M^{(2k+1)}). \tag{57}$$

When $\beta_2/\beta_1\gg 1$, that is, when the beam impinges on the crystal in a direction nearly parallel to the crystal surface, $M\approx\beta_2/\beta_1$ (for $\Sigma_t/\Sigma_s\approx 1$), so

$$N_D^{(2k+1)}(\text{asymptotic}) \approx((2k)!/k!(k+1)!)(\beta_2/\beta_1)^{-1-k}. \tag{58}$$

But since β_2/β is large, the terms $N_D^{(3)}$, $N_D^{(5)}$, $\cdots$ are small compared to $N_D^{(1)}$, so

$$N_D(\text{asymptotic})\approx N_D^{(1)}(\text{asymptotic}). \tag{59}$$

That is, only once-reflected neutrons contribute appreciably to the diffracted current density.

When Σ_t/Σ_s is large, M is large, and the sequence $N_D^{(1)}, N_D^{(3)}, \cdots, N_D^{(2k+1)}, \cdots$ in the asymptotic region decreases very rapidly. Therefore, when the absorption cross section is very large (as is the case for x-ray dif-

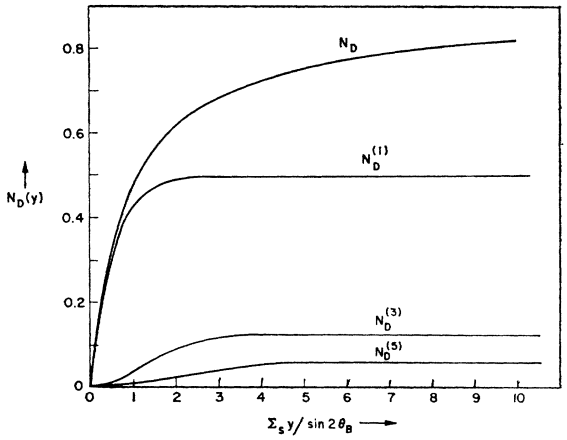

FIG. 16. Plots showing the contributions of the various orders of multiple reflection as a function of position on the surface of a crystal. At large values of y, $N_D\to 1$, showing that once-reflected neutrons contribute only 50% of the total diffracted power.

fraction), the contribution to the diffracted current density by singly reflected particles is predominant.

We can write Eq. (57) in the form

$$N_D^{(2k+1)}(\text{asymptotic})=\frac{(2k)!}{k!(k+1)!}\frac{1}{M}\times\left\{\left(\frac{\Sigma_t}{\Sigma_s}\right)^{2k}\left[\left(\frac{\beta_2}{\beta_1}\right)^{1/2}+\left(\frac{\beta_1}{\beta_2}\right)^{1/2}\right]^{2k}\right\}^{-1}.$$

When $\beta_2 \ll \beta_1$, we see the sequence $N_D^{(1)}$, $N_D^{(3)}$, $\cdots$, $N_D^{(2k+1)}$, $\cdots$ again decreases rapidly, and

$$N_D(\text{asymptotic}) \approx N_D^{(1)}(\text{asymptotic}). \quad (60)$$

Therefore, also in the case where the diffracted beam emerges nearly parallel to the crystal surface (Fankuchen cut), only once-reflected neutrons contribute appreciably to the diffracted current density at the surface of the crystal.

III. CONCLUSIONS

In this paper we have solved the multiple-Bragg-reflection problem in a semi-infinite crystal, and as a result of the analysis are able to state the following conclusions regarding the monochromation of neutrons:

1. The reflected monoenergetic beam peaks at the "effective" right edge of the primary collimator. Consequently, the point on the monochromator surface at which a collimator between the monochromator and the target should "stare" is shifted to the right.
2. It is advantageous to utilize a wide primary collimator so the area of the monochromator from which the exit collimator (which determines the resolution of the system) accepts neutrons is far up on the build-up curves, and consequently, a plane source of "monoenergetic" neutrons can be closely approximated.
3. Cutting the crystal at an angle β causes the diffracted current density to reach its maximum value within a smaller width measured perpendicular to the diffracted beam. However, the *total* number of neutrons reflected by the monochromator decreases with β. Consequently, if one, for some reason, is limited to a given collimator, it might be advantageous to cut the crystal at some angle β in order to obtain a narrow intense beam. The quantitative connection between the angle β and the diffracted beam profile is given explicitly in Sec. II.

A subsequent paper will discuss quantitatively the multiple-Bragg-reflection problem in various crystals of finite dimensions. Particular attention will be given to "slab" crystals placed in both the reflection and transmission positions. We have obtained general solutions to the differential equations given by Hamilton[1] which will be applied to the two problems above which are pertinent to the theory of the monochromation of neutrons. Experimental work on the investigation of the spatial distribution of the diffracted neutron beams from various crystals is currently in progress and will be reported in that paper.

APPENDIX A

We have based the analysis of this paper on the physical picture of a real crystal consisting of many small-angle mosaic grains as originally proposed by Darwin (1922). Assuming that absorption is small and that all of the scattering centers in a given small mosaic grain are bathed in the same incident-wave field (kinematical theory), it is an easy matter to show that the probability for coherent scattering per unit path (for small paths) in a mosaic crystal is

$$\Sigma_s(\theta_0,k)=W(\Delta)Q, \quad (A1)$$

where

$$Q=\frac{(2\pi)^3|F|^2}{V^2k^3\sin 2\theta_B}, \quad (A2)$$

$|F|^2$ = structure factor squared times the Debye-Waller factor, V = volume of a unit cell, $\Delta=\theta_0-\Delta k\tan\theta_B^0$, $W(\Delta)d\Delta$ = number of mosaic grains oriented at angles Δ in $d\Delta$.

The mosaic distribution function $W(\Delta)$ is commonly taken to be Gaussian. A coefficient E_p is generally included in Eq. (A1) in order to correct for primary extinction. Under these assumptions Σ_s takes the form

$$\Sigma_s(\theta_0,k)=E_pQ((2\pi)^{1/2}\eta)^{-1}\times\exp[-(\theta_0-\Delta k\tan\theta_B^0)^2/2\eta], \quad (A3)$$

where $\Delta k\equiv(k/k_B^0-1)$. $\Sigma_t(\theta_0,k)$ is the sum of Σ_s and the linear absorption coefficient μ. The effects of incoherent scattering can be included in μ.